

# Application of Modern Additive Manufacturing Techniques in the Preparation of Flow Models for Optical Flow Measurement Methods

Filip Trnka<sup>1\*</sup>, Hana Schmirlerová<sup>1</sup>, and Martin Májovský<sup>2</sup>

<sup>1</sup>CTU in Prague, Faculty of Mechanical Engineering, Department of Fluid dynamics and Thermodynamics, Technická 4, 160 00 Prague, Czech Republic

<sup>2</sup>Charles University and Military University Hospital, First Faculty of Medicine, Department of Neurosurgery and Neurooncology, U Vojenské nemocnice 1200, 169 02 Prague 6, Czech Republic

**Abstract.** This study presents an experimental methodology for fabricating transparent flow models tailored for Particle Image Velocimetry (PIV). The approach is based on 3D printing complex internal geometries from acrylonitrile styrene acrylate (ASA), a material that can be smoothed using acetone vapours to enhance optical clarity. The ASA models are embedded in Sylgard 184 silicone elastomer and then dissolved in acetone to leave optically transparent flow channels. To evaluate surface treatment effects, stenosis models were divided into sections and subjected to different combinations of sanding and acetone smoothing. Additionally, the method was extended to anatomically accurate nasal cavity models derived from computed tomography (CT) scans. While ASA offers improved surface quality and compatibility with acetone smoothing, the dissolution of complex structures proved time-consuming, taking over 40 days in the nasal model case. Simpler geometries dissolved within two days. Optical clarity and refractive index matching with a glycerol–water solution were sufficient for PIV, though minor mismatches were observed. The findings demonstrate the method’s potential for constructing anatomically realistic, PIV-compatible models, while highlighting trade-offs in preparation time and solvent use. Future work should explore hybrid approaches combining ASA and water-soluble materials like PVA to optimize fabrication efficiency.

## 1 Introduction

In recent years, computational simulations have become increasingly prevalent across a wide range of scientific disciplines. In the field of fluid dynamics, Computational Fluid Dynamics (CFD) has emerged as a well-established and widely used approach for simulating flow behaviour and heat transfer in both academic and applied research contexts. However, as the reliance on CFD simulations grows, the demand for accurate experimental validation becomes more critical than ever [1], [2], [3].

One of the key experimental techniques used for such validation is Particle Image Velocimetry (PIV). This non-intrusive optical measurement method enables the visualization

---

\* Corresponding author: [f.trnka@fs.cvut.cz](mailto:f.trnka@fs.cvut.cz)

and quantification of velocity fields in fluids. The PIV technique is based on tracking the motion of tracer particles within a seeded flow using high-speed cameras. These cameras capture the movement of particles across a plane that is illuminated by a laser sheet, allowing for the reconstruction of the flow field [4], [5].

To perform accurate PIV measurements, certain conditions must be met—most importantly, the use of optically transparent models and a clear optical path for both illumination and image capture. As CFD tools continue to evolve in complexity and precision, they place increased demands on the quality and realism of experimental models used for validation purposes [6].

In response to this need, our research focuses on exploring innovative methods for creating physical flow models, particularly those derived from real patient data such as computed tomography (CT) scans. These models can represent anatomically accurate geometries such as the nasal cavities of patients who have undergone medical interventions enabling detailed investigation of internal airflow dynamics [6], [7], [8].

To achieve this, we have established a methodology in our laboratory that combines 3D printing with casting techniques. Specifically, we use water-soluble polyvinyl alcohol (PVA) to 3D print internal flow geometries. These printed models are then embedded within a transparent polymer casting. Once the polymer has cured, the PVA core is dissolved, leaving behind a hollow internal structure suitable for optical measurements using PIV [6].

This approach provides a flexible and cost-effective way to create anatomically realistic, optically clear flow models that are well-suited for experimental fluid dynamics studies, particularly those requiring validation of CFD simulations in complex geometries [6].

## 2 Methods

### 2.1 Experimental models

Stenosis models described in [6] were fabricated using polyvinyl alcohol (PVA) material. As a surface treatment, manual sanding was applied to improve smoothness. The printed models were then embedded in Plexiglas moulds, into which Sylgard 184 silicone elastomer was poured. After the silicone solidified, the PVA models were dissolved using water, resulting in a hollow cavity that replicated the stenosis geometry within a solid transparent block.

For the purposes of this study, we modified the model preparation procedure presented in [6]. Specifically, the models were printed using acrylonitrile styrene acrylate (ASA), a material that is soluble in acetone and its vapours. The diameters of the modified models are shown in Figure 1. A key advantage of ASA is its ability to undergo surface smoothing through exposure to acetone vapours, as documented in [9], [10].

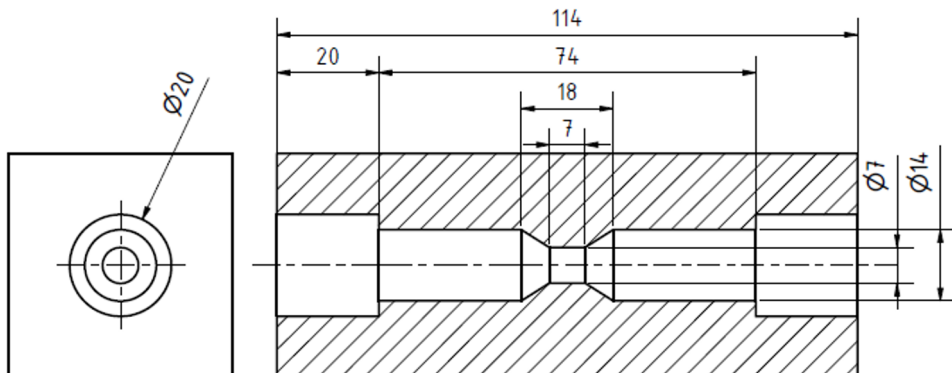


**Fig. 1.** Diameters of stenosis model.

## 2.2 3D printing and surface treatment

Two stenosis models were printed based on the diameters shown in Figure 1. Each model was divided into two sections, with different surface treatments applied to evaluate their influence on optical clarity and surface finish. The models were fabricated using a Prusa MK3S 3D printer equipped with a 0.4 mm bronze nozzle. The printing was carried out using Prusament ASA Galaxy Black filament with a layer height of 0.15 mm. The nozzle temperature was set to 250 °C and the print bed was maintained at 90 °C.

Figure 2 illustrates the four surface treatment methods, which are further detailed in Table 1. Section B remained untreated and serves as a reference. Section A was manually brushed with acetone to smooth the surface. Section C was first hand-sanded using P140 sandpaper for approximately 3 minutes and subsequently exposed to acetone vapours for two hours at room temperature (20 °C). Section D was treated only with acetone vapor smoothing under the same conditions.

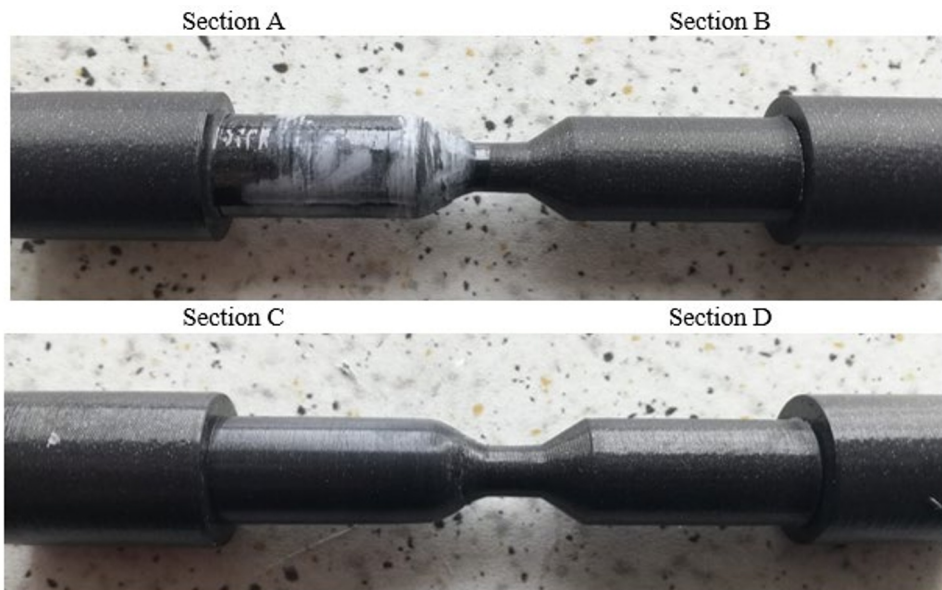


**Fig. 2.** Different sections of stenosis models.

**Table 1.** Surface treatment on different sections.

Section	Operation
A	Painted with acetone by brush
B	Without any treatment
C	Hand sanded, with 140 grid paper + smoothing by acetone vapours
D	Smoothing by acetone vapours

## 2.3 Casting and dissolution

Sylgard 184 is a silicone elastomer with excellent optical properties and is well-suited for PIV due to its refractive index being close to that of a water–glycerol solution [6].

The printed stenosis models were inserted into custom-made Plexiglas moulds, and Sylgard 184 was poured in to fully encapsulate the geometry. The standard curing time of Sylgard 184 at room temperature is several hours; however, this process can be significantly

accelerated at elevated temperatures. At 120 °C, the material cures in approximately 30 minutes.

In our procedure, the filled moulds were left to rest overnight at room temperature to allow air bubbles to escape naturally. The next day, the moulds were placed in a preheated oven and cured at 120 °C for 40 minutes to ensure complete polymerization. Figure 3 shows the fully cured models within their Plexiglas moulds, still containing the internal ASA stenosis structures.

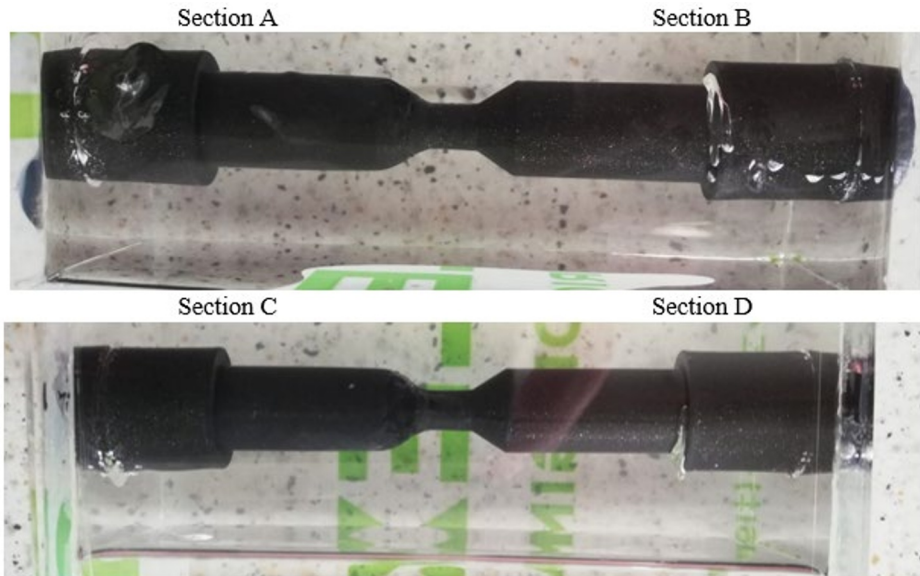


**Fig. 3.** Cured Sylgard models with stenosis.

The next step involved dissolving the stenosis models in order to create transparent flow channels shaped by the internal geometry, suitable for PIV measurements. After curing, the Sylgard blocks were carefully removed from the Plexiglas moulds and placed into a sealed glass container filled with acetone. The ASA material gradually dissolved, leaving behind a hollow cavity corresponding to the original stenosis geometry. Long exposure of cured Sylgard to acetone was experimentally tested. Acetone is able to diffuse in and out of the Sylgard without any changes to the Sylgard.

## 2.4 Models of complex geometries

The same methodology as described for Section D was applied to create a model of human nasal cavities from ASA material, representing a more complex internal geometry. Model of nasal cavities were prepared based on CT scans of patient [8]. To ensure fully developed flow at the inlet, entrance lengths were added to the model. These segments were printed from water-soluble PVA in order to reduce the total dissolution time.

Figure 4A shows the nasal cavity model encapsulated in transparent Sylgard prior to dissolving the 3D-printed parts, while Figure 4B shows the resulting flow channel after the ASA and PVA materials were fully removed.

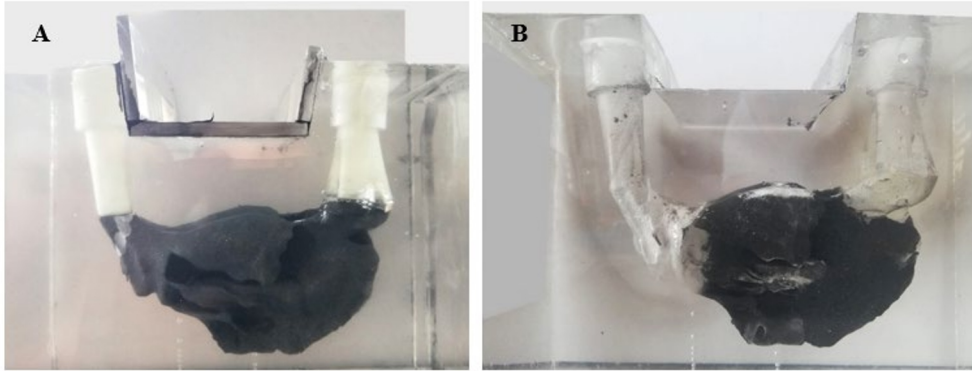


**Fig. 4.** Complex 3D printed nasal cavity in Sylgard model; A – before dissolving; B – in process of dissolving.

### 3 Results

For PIV measurements, it is crucial to match the refractive index of the model material with that of the working fluid to minimize optical distortions. Another key factor is the optical clarity of the model, which directly affects image quality and particle tracking accuracy. Figure 5 shows the model after dissolution of the 3D-printed ASA stenosis, filled with a glycerol–water solution (60.07% by weight). The refractive index of the solution was measured as  $n = 1.4067 \pm 0.0003$  and dynamic viscosity was  $\mu = (11,000 \pm 0,011)$  mPas. Red lines have been added to highlight the region containing the internal cavity shaped by the stenosis geometry. All four surface treatment sections are displayed for comparison.

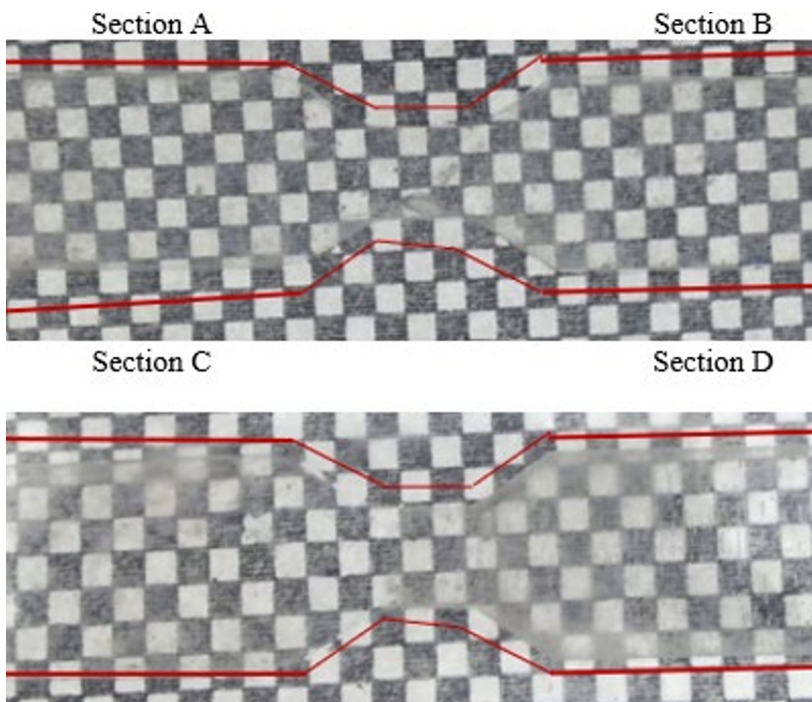


**Fig. 5.** Sections of stenosis models - after dissolving ASA.

## 4 Discussion

Figure 5 shows the interaction between the glycerol–water solution and the Sylgard model. In our laboratory, we use these two materials together to minimize the difference in refractive index and improve optical clarity. However, in the case presented, a visible mismatch was observed. This discrepancy may be attributed to two main factors. First, the refractive index of Sylgard is  $n = 1.4122$ , while the prepared glycerol–water solution had a refractive index of  $n = 1.4067$ , indicating a slight mismatch. Second, the surface treatment may have been insufficient, or the surface quality may have been affected during the dissolution process of the ASA model.

Despite the mismatch, the overall optical clarity appears sufficient for PIV measurements. Minor differences in refractive index can still allow for accurate velocity field acquisition, depending on the camera optics, laser sheet configuration, and seeding particle size.

Figure 4 illustrates the production of a more complex model representing a nasal cavity, which are still in process of dissolving 3D printed parts. Dissolving the 3D-printed ASA and PVA material from this model required over 40 days, involving repeated additions of acetone and mechanical extraction of residual material. This highlights a significant limitation in applying this method to geometrically complex models. In contrast, the simpler stenosis models were successfully dissolved within two days, with ASA softened sufficiently for careful removal without damaging the Sylgard matrix.

## 5 Conclusion

The dissolution time of printed materials is a critical factor when considering the use of this method for future applications. A major advantage of using ASA is the ability to easily smooth the surface using acetone vapours, which improves optical properties and can enhance PIV measurement quality.

However, a significant drawback is the long dissolution time required after Sylgard curing, particularly for complex geometries. This introduces considerable delays and increases the amount of acetone consumed. In contrast, water-soluble materials like PVA offer a faster and more environmentally friendly alternative for certain model segments.

Using ASA as a material for 3D printing internal flow models is feasible, but further work is needed to define detailed protocols for surface treatment and dissolution. Consideration must also be given to the time required for model preparation and the operational costs associated with acetone use when compared to water-based alternatives.

### Acknowledgments

This work was supported by the Grant Agency of the Czech Technical University in Prague, under Grant No. SGS25/128/OHK2/3T/12; Ministry of Defence of the Czech Republic under Grant No. MO1012; Ministry of Health of the Czech Republic under Grant No. NW24-08-00324; and Cooperation Neuroscience Charles University.

## References

1. N.L. Phuong, K. Ito, Investigation of flow pattern in upper human airway including oral and nasal inhalation by PIV and CFD, *Build Environ*, vol. **94**, pp. 504–515, Dec. 2015. <https://doi.org/10.1016/j.buildenv.2015.10.002>
2. J. Ormiskangas et al., Assessment of PIV performance in validating CFD models from nasal cavity CBCT scans, *Respir Physiol Neurobiol*, vol. **282**, Nov. 2020. <https://doi.org/10.1016/j.resp.2020.103508>
3. S.K. Kim, Y. Na, J.I. Kim, S.K. Chung, Patient specific CFD models of nasal airflow: Overview of methods and challenges, *J Biomech*, vol. **46**, no. 2, pp. 299–306, Jan. 2013. <https://doi.org/10.1016/j.jbiomech.2012.11.022>
4. A. Lecuona, J. Nogueira, P.A. Rodríguez, A. Acosta, PIV evaluation algorithms for industrial applications, *Meas Sci Technol*, vol. **15**, no. 6, pp. 1027–1038, 2004. [doi:10.1088/0957-0233/15/6/001](https://doi.org/10.1088/0957-0233/15/6/001)
5. F.G. Ergin, J. Olofsson, P. Petersson, N.F. Gade-Nielsen, A hybrid phase boundary detection technique for two-phase-flow PIV measurements, *Flow Measurement and Instrumentation*, vol. **74**, Aug. 2020. <https://doi.org/10.1016/j.flowmeasinst.2020.101776>
6. A. Bláha, A. Kuzmíková, F. Trnka, Mutual interaction of serially arranged stenoses at low Reynolds numbers. *AIP Conf. Proc.* 14 February 2023; 2672 (1): 030021. <https://doi.org/10.1063/5.0133006>
7. F. Trnka, H. Schmirlerová, M. Májovský, D. Netuka, M. Schmirler, Examining the Impact of Inlet Shape on Nasal Cavity Flow Field: A Computational Investigation, *MATEC Web of Conferences*, vol. **383**, p. 00021, Oct. 2023. <https://doi.org/10.1051/mateconf/202338300021>
8. F. Trnka, H. Schmirlerová, M. Májovský, D. Netuka, M. Schmirler, Preparation of a Real Model of Nasal Cavities from Computed Tomography for Numerical Simulation, *MATEC Web of Conferences*, vol. 369, p. 01005, 2022. <https://doi.org/10.1051/mateconf/202236901005>
9. J. S. Chohan, R. Singh, K. S. Boparai, Vapor smoothing process for surface finishing of FDM replicas, in *Materials Today: Proceedings*, Elsevier Ltd, 2019, pp. 173–179. <https://doi.org/10.1016/j.matpr.2019.09.013>
10. R. Singh, S. Singh, I.P. Singh, F. Fabbrocino, F. Fraternali, Investigation for surface finish improvement of FDM parts by vapor smoothing process, *Compos B Eng*, vol. 111, pp. 228–234, Feb. 2017. <https://doi.org/10.1016/j.compositesb.2016.11.062>